

Supporting Information

Free-standing hybrid films based on graphene and porous carbon particles for flexible supercapacitors

Guillermo A. Ferrero, Marta Sevilla, and Antonio B. Fuertes*

Instituto Nacional del Carbón (CSIC), P.O. Box 73, Oviedo 33080, Spain

*Corresponding author: abefu@incar.csic.es

Preparation of the carbon nanosheets¹

In a typical synthesis procedure, 5 g of potassium citrate (Aldrich) was heat-treated in a stainless steel reactor under nitrogen up to 850 °C at a heating rate of 3 °C min⁻¹ and held at this temperature for 1 h. The black solid residue was then washed with HCl (10%). Finally, the solid was collected by filtration, washed with abundant distilled water, and dried at 120 °C for several hours. The carbon samples were denoted as CK.

Preparation of the carbon microspheres²

Synthesis of the hydrochar materials: Hydrochar materials were prepared by the hydrothermal carbonization of α-D-Glucose (96 %, Aldrich). Briefly, an aqueous solution of the raw material (0.25 M) was placed in a Teflon-lined stainless-steel autoclave, heated up to 180 °C, and kept at this temperature for 5 h. The resulting carbonaceous solids (hydrochars) were recovered by centrifugation, washed with distilled water, and dried at 120 °C for several hours.

Synthesis of porous carbon materials: The hydrochar material was added to a dispersion that contained KHCO₃ and melamine (KHCO₃/hydrochar weight ratio=6 and melamine/hydrochar weight ratio=2). After the evaporation of the water (under magnetic stirring), the resulting mixture was heat-treated up to 800 °C (heating rate: 5 °Cmin⁻¹) under a N₂ gas flow and held at this temperature for 1 h. The activated carbon thus synthesized was denoted as CS.

Table S1. Chemical composition and distribution of the carbon functional groups.

Functional groups (%)	Sample Code		
	GP	GP-CK	GP-CS
C-C sp ²	55.6	54.6	57.9
C-C sp ³	23.2	22.4	22.1
C in carbonyl (C=O)	8.3	7.9	7.5
C-O	8.5	8.6	7.5
O-C=O	2.9	4.1	3.4
π-π* shake-up satellite	1.5	2.4	1.6

Table S2. Comparison of the cell areal capacitance for supercapacitors based on graphene films and hybrid graphene films reported in the literature (two-electrode cell system).

Material	Electrolyte	Areal cell capacitance (mF cm^{-2})		Reference
		Low discharge rates	High discharge rates	
GP	1 M H_2SO_4	103 (0.23 mA cm^{-2})	70 (1190 mA cm^{-2})	This work
GP-CK	1 M H_2SO_4	136.2 (0.23 mA cm^{-2})	80 (1380 mA cm^{-2})	This work
GP-CS	1 M H_2SO_4	160 (0.29 mA cm^{-2})	103 (1242 mA cm^{-2})	
Graphene-cellulose paper	1 M H_2SO_4	41	23	3
Graphene gel	1 M H_2SO_4	33.8 (1 mA cm^{-2})	26.4 (100 mA cm^{-2})	4
Solvated Graphene Film	1 M H_2SO_4	48 (0.045 mA cm^{-2})	35 (486 mA cm^{-2})	5
Holey Graphene Paper	1 M H_2SO_4	104.5 (1 mA cm^{-2})	78.5 (20 mA cm^{-2})	6
Graphene Hydrogel Films	1 M H_2SO_4	190 (2 mA cm^{-2})	152 (20 mA cm^{-2})	7
Hierarchical Porous Graphene Films	1 M H_2SO_4	71 (1 mA cm^{-2})	54.7 (100 mA cm^{-2})	8
Chemically converted graphene hydrogel films	1 M H_2SO_4	95 (0.1 mA cm^{-2})	50 (200 mA cm^{-2})	9
Crumpled Graphene Papers	1 M H_2SO_4	81	58 (57.6 mA cm^{-2})	10
Functionalized Graphene Hydrogel Film	1 M H_2SO_4	225	175 (20 mA cm^{-2})	11
RGO-PPy membrane	2 M KCL	175 (1 mV s^{-1})	125 (400 mV s^{-1})	12
Graphene/Polyaniline/Graphene Nanocomposite Paper	1 M H_2SO_4	290 (1 mA cm^{-2})	187 (10 mA cm^{-2})	13
Flexible graphene paper pillared by carbon black	6 M KOH	19.3 (10 mV s^{-1})	11.4 (500 mV s^{-1})	14
Graphene-CMK-5	6 M KOH	178.5 (0.6 mA cm^{-2})	-	15
Multifunctional aerogel	6 M KOH	77.5 (0.2 mA cm^{-2})	38.8 (70 mA cm^{-2})	16

Table S3. Comparison of the cell areal capacitance for solid-state supercapacitors assembled with graphene films and hybrid graphene films reported in the literature.

Material	Electrolyte	Areal cell capacitance (mF cm^{-2})		Reference
		Low discharge rates	High discharge rates	
GP	H_2SO_4 -PVA	108.1 (0.26 mA cm^{-2})	91 (52.2 mA cm^{-2})	This work
GP-CS	H_2SO_4 -PVA	165 (0.52 mA cm^{-2})	96 (51.7 mA cm^{-2})	This work
Graphene-cellulose paper	H_2SO_4 -PVA	46 (2 mV s^{-1})	-	3
Holey Graphene Paper	H_2SO_4 -PVA	100.5 (1 mA cm^{-2})	70 (20 mA cm^{-2})	6
Graphene Hydrogel Films	H_2SO_4 -PVA	372 (2 mA cm^{-2})	260 (40 mA cm^{-2})	7
Functionalized Graphene Hydrogel Film	H_2SO_4 -PVA	206 (1 mA cm^{-2})	152 (20 mA cm^{-2})	11
Graphene/ Polyaniline/Graphene Nanocomposite Paper	H_2SO_4 -PVA	121 (0.2 mA cm^{-2})	75 (10 mA cm^{-2})	13
Graphene nanosheets incorporated hierarchical porous carbon	H_2SO_4 -PVA	76.1 (10 mA cm^{-2})	30 (30 mA cm^{-2})	17
Electrochemically exfoliated Graphene and nanoporous activated graphene	H_2SO_4 -PVA	89.5 (10 mV s^{-1})	40.4 (1000 mV s^{-1})	18
Cellulose nanofiber-graphene	H_2SO_4 -PVA	158	-	19
Polypyrrole-coated paper	H_3PO_4 -PVA	420 (1 mA cm^{-2})	230 (20 mA cm^{-2})	20

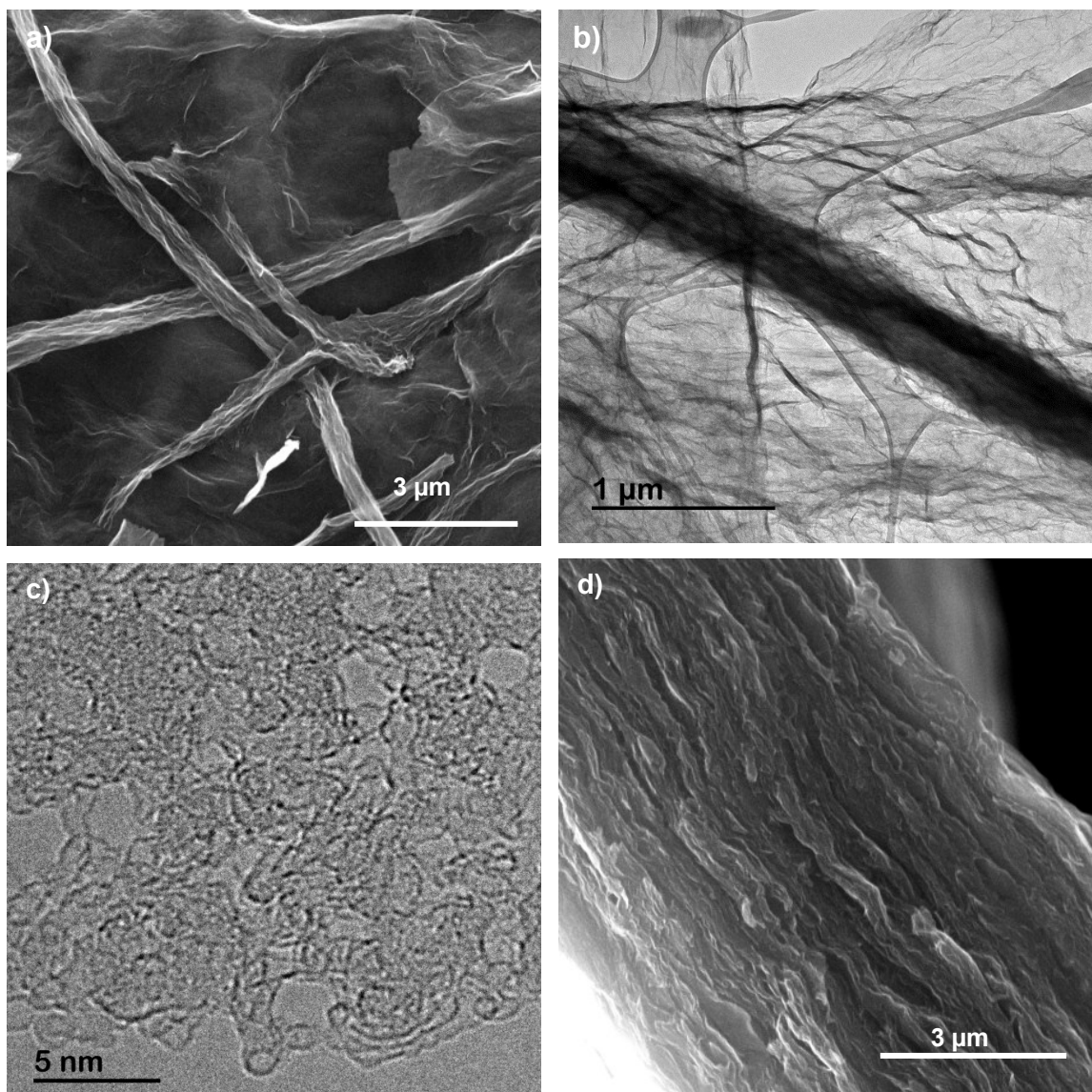


Figure S1. (a) SEM and, (b) TEM images of a wrinkled graphene sheet and a graphene nanoscroll, (c) HRTEM image of a graphene sheets showing the in-plane nanopores and (d) a cross-section figure of the GP paper.

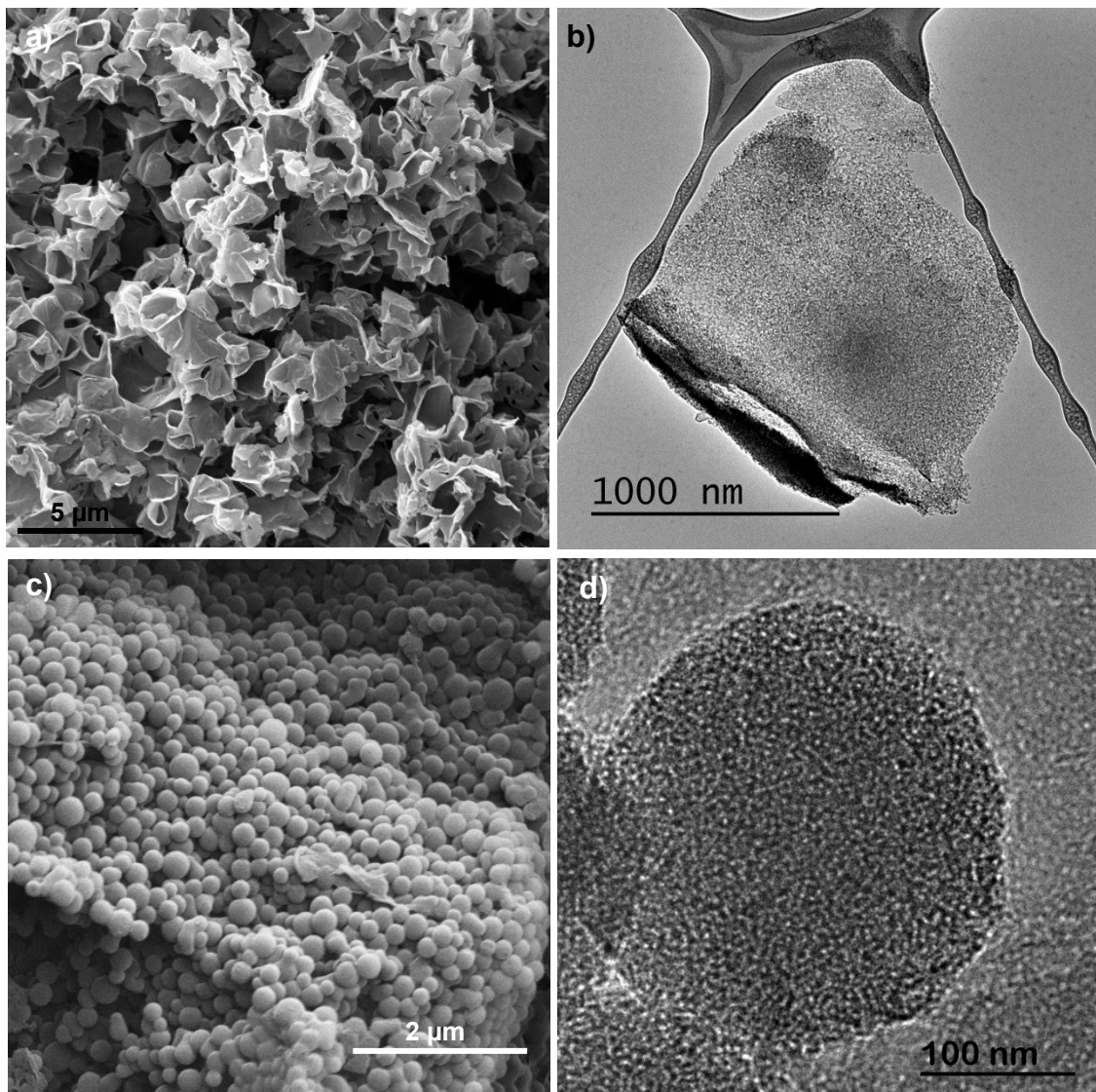


Figure S2. SEM and TEM images of CK (a, b) and CS (c, d) carbon particles.

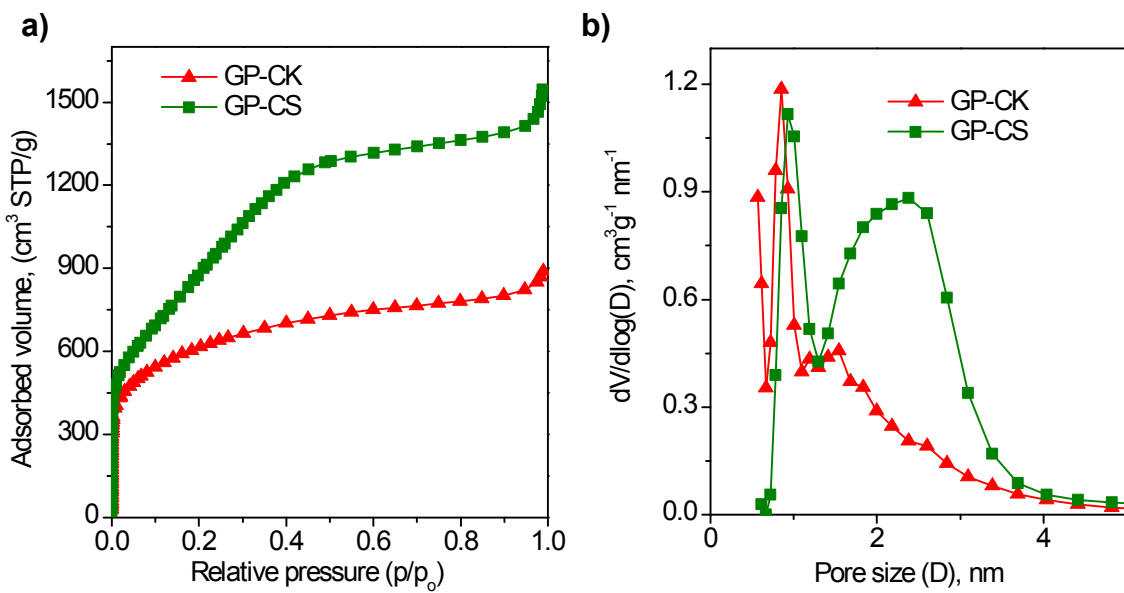


Figure S3. (a) Nitrogen sorption isotherms and (b) pore size distributions deduced by means of the QSDFT method for the CK and CS porous carbon samples.

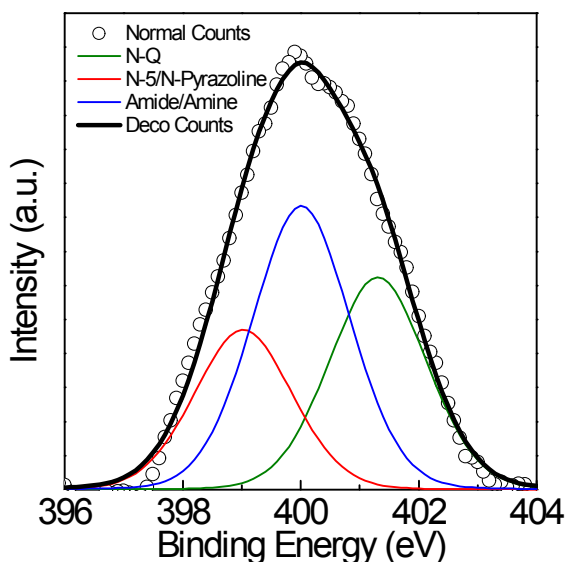


Figure S4. High-resolution XPS N1s spectrum of the GP-CS paper.

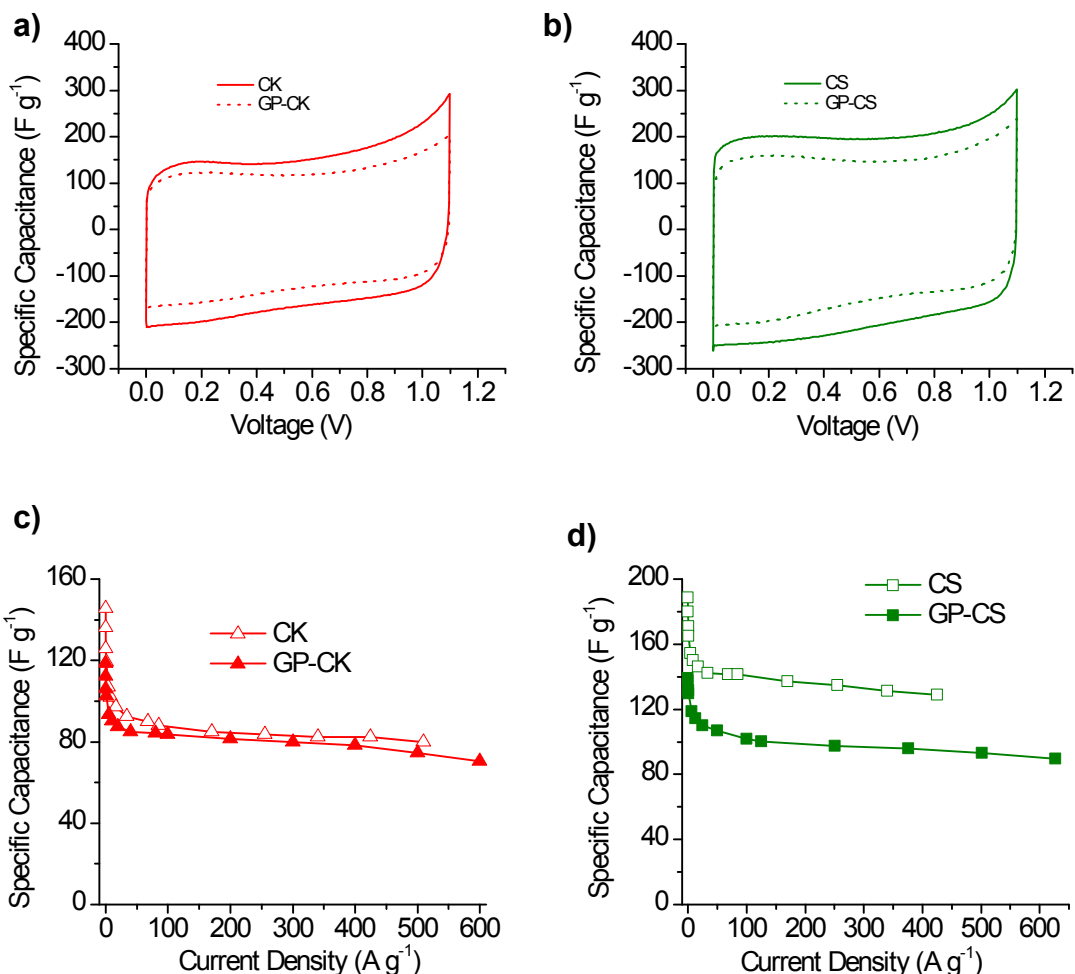


Figure S5. Cyclic voltammograms at 5 mV s^{-1} for (a) the CK and GP-CK samples and (b) the CS and GP-CS samples, and variation of the electrode gravimetric capacitance with the current density for (c) the CK and GP-CK samples and (d) the CS and GP-CS samples. Electrolyte: $1 \text{ M H}_2\text{SO}_4$.

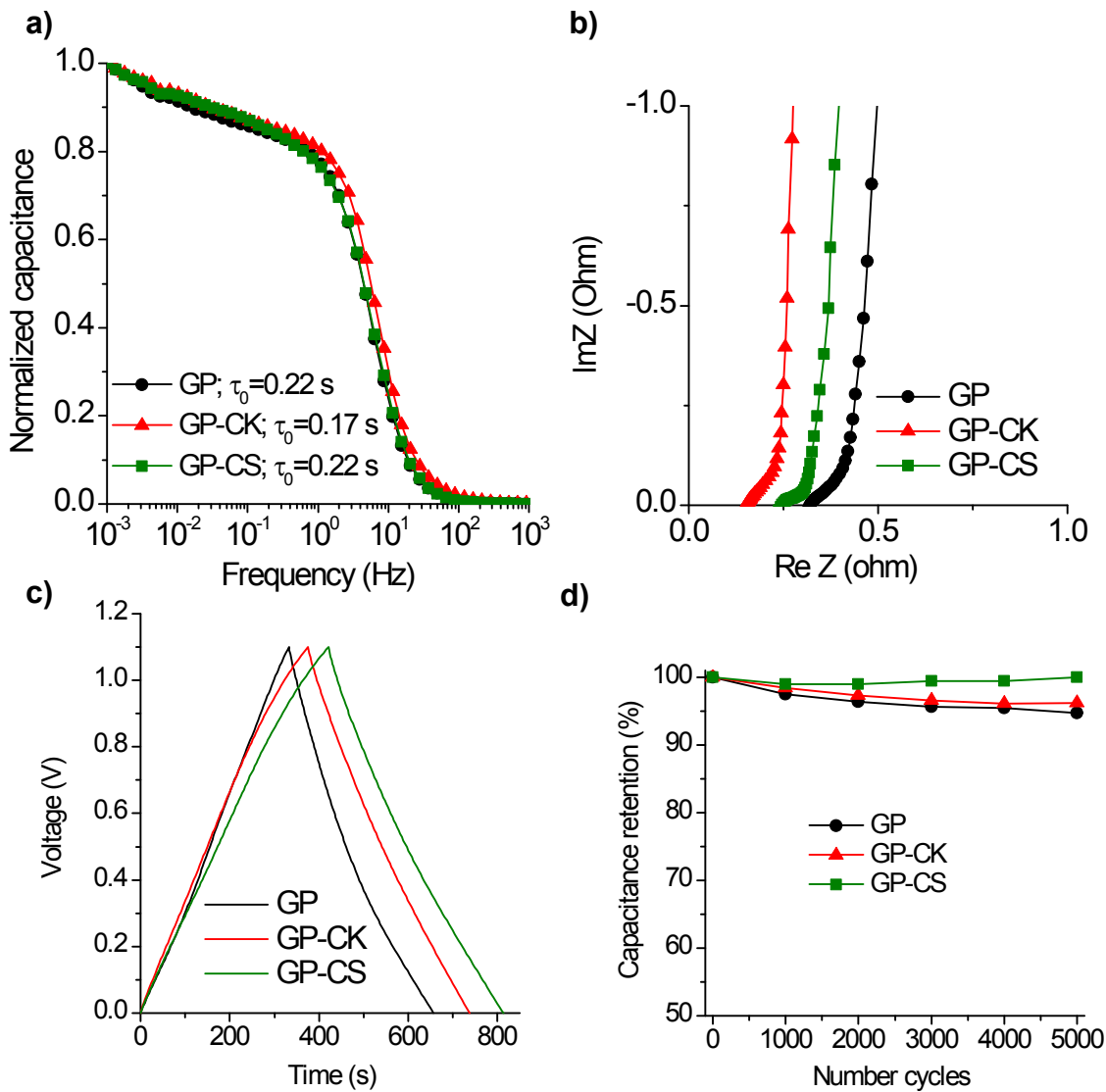


Figure S6. (a) Bode plot, (b) Nyquist plot, (c) galvanostatic charge-discharge cycles at $\sim 0.5 \text{ mA cm}^{-2}$ and (d) long-term cycling stability at 12 mA cm^{-2} for the supercapacitors assembled with the GP, GP-CK and GP-CS papers. Electrolyte: $1 \text{ M H}_2\text{SO}_4$.

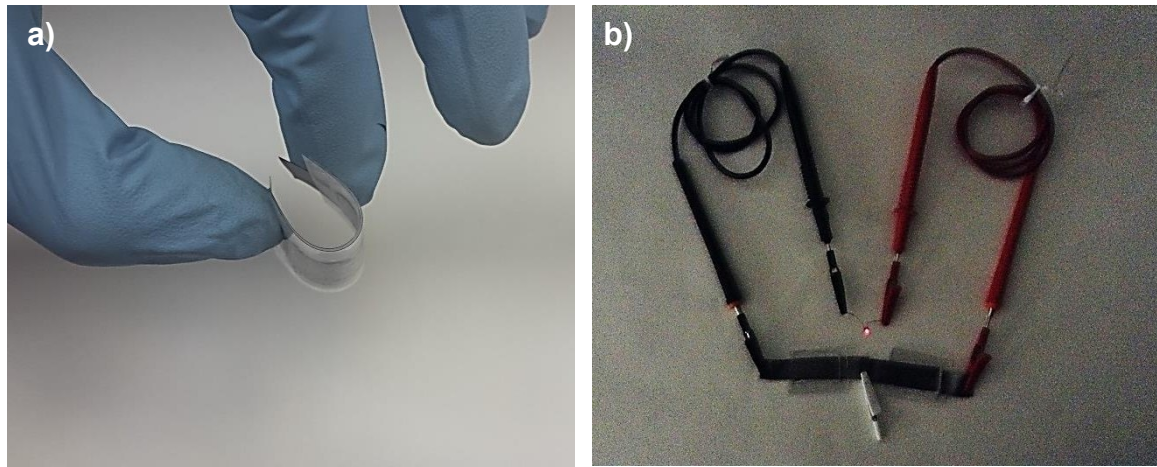


Figure S7. (a) Image of the solid-state supercapacitor device and (b) a red LED lit by two flexible supercapacitors connected in series. Electrode material GP-CS.

References

1. M. Sevilla and A. B. Fuertes, *ACS Nano*, 2014, **8**, 5069-5078.
2. M. Sevilla and A. B. Fuertes, *ChemSusChem*, 2016, **9**, 1880-1888.
3. Z. Weng, Y. Su, D.-W. Wang, F. Li, J. Du and H.-M. Cheng, *Adv. Energy Mater.*, 2011, **1**, 917-922.
4. U. N. Maiti, J. Lim, K. E. Lee, W. J. Lee and S. O. Kim, *Adv. Mater.*, 2014, **26**, 615-619.
5. X. Yang, J. Zhu, L. Qiu and D. Li, *Adv. Mater.*, 2011, **23**, 2833-2838.
6. Y. Xu, C.-Y. Chen, Z. Zhao, Z. Lin, C. Lee, X. Xu, C. Wang, Y. Huang, M. I. Shakir and X. Duan, *Nano Letters*, 2015, **15**, 4605-4610.
7. Y. Xu, Z. Lin, X. Huang, Y. Liu, Y. Huang and X. Duan, *ACS Nano*, 2013, **7**, 4042-4049.
8. Z. Xiong, C. Liao, W. Han and X. Wang, *Adv. Mater.*, 2015, **27**, 4469-4475.
9. X. Yang, C. Cheng, Y. Wang, L. Qiu and D. Li, *Science*, 2013, **341**, 534-537.
10. J. Zang, C. Cao, Y. Feng, J. Liu and X. Zhao, *Sci. Rep.*, 2014, **4**, 6492.
11. Y. Xu, Z. Lin, X. Huang, Y. Wang, Y. Huang and X. Duan, *Adv. Mater.*, 2013, **25**, 5779-5784.
12. J. Zhang, P. Chen, B. H. L. Oh and M. B. Chan-Park, *Nanoscale*, 2013, **5**, 9860-9866.
13. F. Xiao, S. Yang, Z. Zhang, H. Liu, J. Xiao, L. Wan, J. Luo, S. Wang and Y. Liu, *Sci. Rep.*, 2015, **5**, 9359.
14. G. Wang, X. Sun, F. Lu, H. Sun, M. Yu, W. Jiang, C. Liu and J. Lian, *Small*, 2012, **8**, 452-459.
15. Z. Lei, Z. Liu, H. Wang, X. Sun, L. Lu and X. S. Zhao, *J. Mater. Chem. A*, 2013, **1**, 2313-2321.
16. J. Zhu, X. Yang, Z. Fu, J. He, C. Wang, W. Wu and L. Zhang, *Chemistry – A European Journal*, 2016, **22**, 2515-2524.
17. Z. Zhu, H. Jiang, S. Guo, Q. Cheng, Y. Hu and C. Li, *Sci. Rep.*, 2015, **5**, 15936.
18. Z.-S. Wu, S. Yang, L. Zhang, J. B. Wagner, X. Feng and K. Müllen, *Energy Storage Materials*, 2015, **1**, 119-126.
19. K. Gao, Z. Shao, J. Li, X. Wang, X. Peng, W. Wang and F. Wang, *J. Mater. Chem. A*, 2013, **1**, 63-67.
20. L. Yuan, B. Yao, B. Hu, K. Huo, W. Chen and J. Zhou, *Energy Environ. Sci.*, 2013, **6**, 470-476.